Mater. Res. Soc. Symp. Proc. Vol. 1728 © 2015 Materials Research Society
DOI: 10.1557/opl.2015.357

# Enhanced selective thermal emission with a meta-mirror following Generalized Snell's Law

M. Ryyan Khan[1], Xufeng Wang[1], Enas Sakr[1], Muhammad A. Alam[1], and Peter Bermel[1,2]
[1]School of Electrical and Computer Engineering, West Lafayette, IN 47907, U.S.A.
[2]Birck Nanotechnology Center, West Lafayette, IN 47907, U.S.A.

## ABSTRACT
Thermal emission plays a critical role in a wide variety of applications, including adjusting radiative losses in photovoltaics and selective solar absorbers, as well as enhancing the emission of high energy photons for thermophotovoltaics and photon-enhanced thermionic emission. In this work, we consider the benefit to thermal emission associated with replacing conventional mirrors with meta-mirrors following Generalized Snell's Law. By reflecting light at a different angle than incident, they can couple internally guided thermal radiation modes to the escape cone, ideally starting from any internally-guided angle. We illustrate the concept with two meta-mirror structures: a graded index material and a xylophone structure. Even without optimization, angle-averaged selective thermal emission is significantly enhanced compared to the planar case at selected wavelengths. Furthermore, the central wavelength and bandwidth of the enhancement can be matched with the requirements of each application.

## INTRODUCTION
The selective enhancement of radiative thermal emission is an emerging scientific theme in a wide variety of applications, including photovoltaics (PV), selective solar absorbers (SSA), thermophotovoltaics (TPV), and photon-enhanced thermionic emission (PETE), as shown in Fig. 1. For instance, photovoltaic cells could benefit from radiative cooling [1,2], particularly in indirect bandgap materials such as crystalline silicon [3]. Selective solar absorbers benefit from the simultaneous ability to emit little in the mid-infrared as they heat up, while trapping solar wavelengths in the visible and near-IR [4,5]. In terms of selective thermal emission, both TPV [6] and PETE [7] benefit from strong emission above a certain energy. While the efficiency of solid state energy conversion has reached 23% at 970 °C for TPV [8] and 2% at 120 °C for PETE [7], researchers have yet to realize the full potential of these technologies, which is more than twice as high. The efficiencies of PV, SSA, TPV, and PETE are all dependent on the precise operating temperatures of both the photon sources and receivers, as well as the wavelengths of light exchanged. Certain wavelengths, generally close to

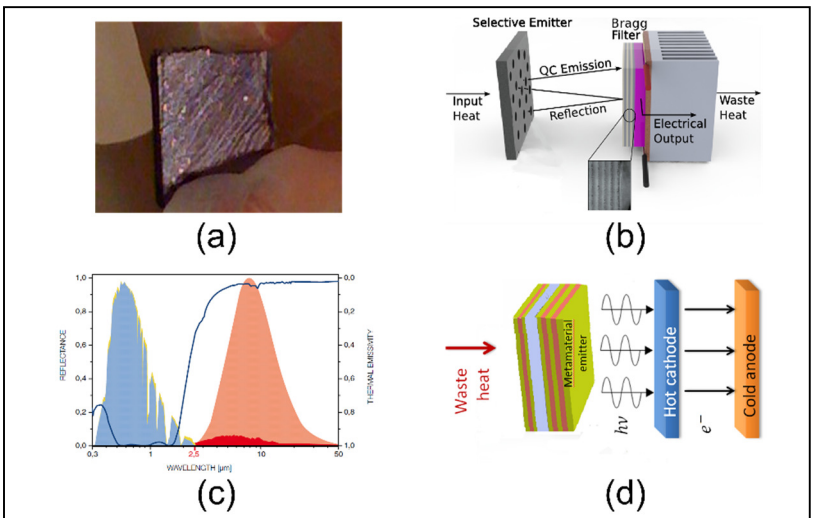


Fig. 1: Potential applications for selective enhancement of thermal emission include: (a) photovoltaics [3], (b) thermophotovoltaics (TPV) [6], (c) selective solar absorbers [4], and (d) photon-enhanced thermal emitters (PETE) [7].

the semiconductor band edge, will yield high performance, whereas most other wavelengths will have a much lower or even zero response. In all these cases, a primary cause of the substantial performance gap between theory and experiment is insufficient control over the thermal emission spectrum.

In order to address the need for selective enhancement of emission for key wavelengths, a variety of approaches have been tried. Originally, the geometric light scattering approach was used, in which thermally generated light is randomly scattered over a broad range of angles inside a high-index material, with a mirror on the bottom to force emission into a single direction. This approach was shown to yield an enhancement factor up to $4n^2$, where $n$ is the refractive index of the absorbing medium [9]. In addition, random scattering structures must generally have thicknesses of at least multiple wavelengths for the best performance [10,11].

However, introducing nanoscale features for light trapping means that the previous limits, derived under the assumptions of classical optics, no longer apply. Instead, wave optics dictates new limits; it has been shown to be capable, in principle, of outperforming all geometrical optics approaches, for enhancements exceeding $4n^2$ [3,12]. This is particularly true over narrow bandwidths, because, in contrast to geometrical optics approaches that treat all wavelengths of light equally, wave optics approaches can be targeted to enhance emission enhancement only in the range where it can be most beneficial. However, it has been shown that there are also new limits to the bandwidth and absolute degree to which emission can be enhanced. The major strategy for light trapping that has emerged recently is using periodic media such as gratings and photonic crystals, which strongly interact with light in key wavelengths of the blackbody spectrum. However, a single periodic structure does not yield the maximum possible enhancement at every wavelength of interest.

Further major advances in selective emitter performance are likely to arise from entirely new techniques for enhanced emission. One approach of great interest since 2011 is the use of metasurfaces, illustrated in Fig. 2. Originally demonstrated by Nanfang Yu *et al*. at Harvard [13], these structures impart a phase across a flat dielectric. As explored in this manuscript, that simple change could have tremendous implications for the performance of these devices.

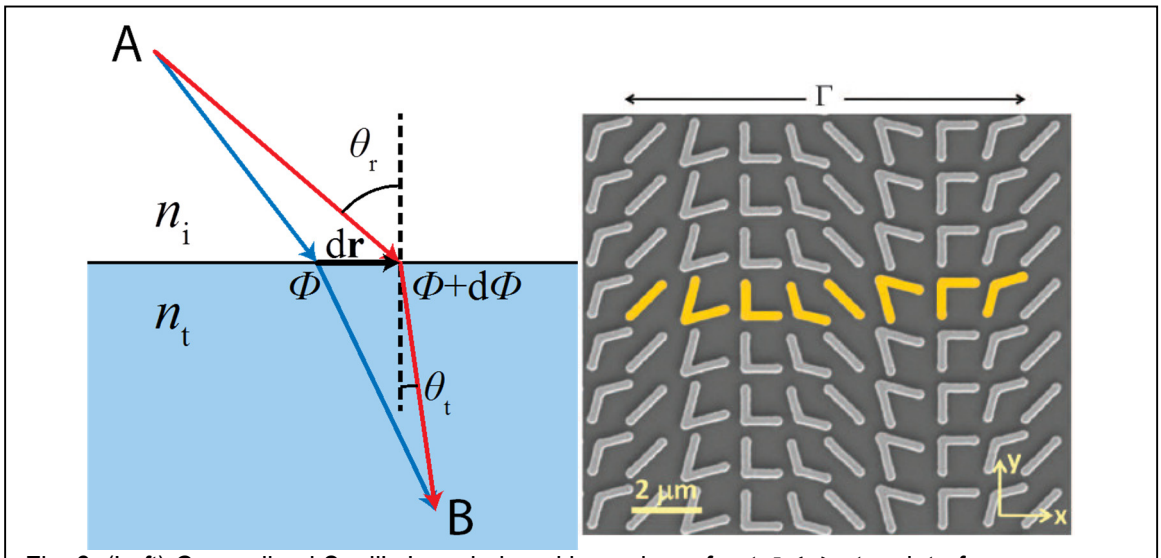


Fig. 2: (Left) Generalized Snell's Law, induced by a phase front $\Phi(\boldsymbol{r})$ at an interface. (Right) Metasurface fabricated by Nanfang Yu *et al*., demonstrating Generalized Snell's law behavior at infrared wavelengths (adapted from [13]).

## THEORY

In this paper, we will study an ultrathin metasurface structure that will strongly enhance the photon density of states and emission in the infrared. It can be shown that the overall emission depends as much on the photon density of states, driven by the effective refractive index of the material, as much as the absorption coefficient itself. An example of these types of structures is given in Fig. 2(a), where a gradient in an ultra-thin layer of thickness $t < 20$ nm introduces a phase front for incoming light. These structures create a significant bias for light to be externally emitter outside the absorber layer of the structure. The effect of such surfaces will be simulated using both the Stanford Stratified Structure Solver, a rigorous coupled-wave technique [14,15], as well as MEEP, a finite-difference time-domain solver [16].

Consider a 'meta-mirror' which adds a phase shift $\Phi(x)$ at any point $x$ on the mirror surface upon reflection of the incident wave. This is known as the 'Generalized Snell's Law' of reflection. This asymmetric scattering offers the possibility of strong enhancement of emission or absorption [17].

In the special case when $\Phi(x)$ varies linearly with $x$, we have $\Delta k_x = d\Phi(x)/dx =$ constant. This can be viewed as an addition of a constant tangential $k$-component $\Delta k_x$ to the incident plane wave such that the angle of reflection will not equal the angle of incidence, as would be expected from the conventional Snell's Law of reflection. We can write this relationship as follows:

$$k_0 n \sin\theta_r = k_0 n \sin\theta_i + \Delta k_x \tag{1}$$

$$\theta_r = \operatorname{asin}\left(\sin\theta_i + \frac{\Delta k_x}{k_0 n}\right) = \operatorname{asin}(\sin\theta_i + \delta) \tag{2}$$

Instead, the mirror effectively steers internally emitted plane waves outside the escape cone, where $\sin\theta_i \geq (1 - \delta)$, into different angles.

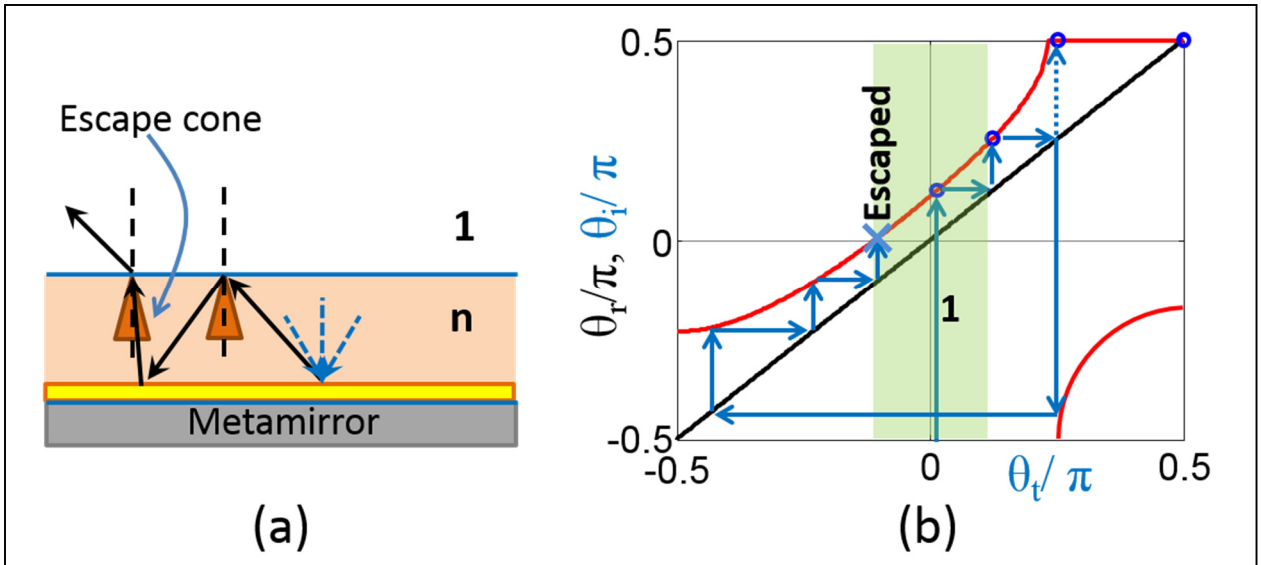


Fig. 3: (a) Our metasurface concept for selective enhancement of emission is shown. A dielectric with refractive index $n$ is placed on top of a meta-mirror which follows the Generalized Snell's law of reflection. The meta-mirror shown here combines a gradient phase adding interface layer with a perfect mirror. A path for the light ray is calculated by ray tracing. (b) The red line shows reflection at the meta-mirror, and the black line represents specular reflection. The shaded region represents the escape cone.

Fig. 3(a) shows the mechanism for the enhancement of thermal emission. For a conventional air-dielectric-mirror configuration, thermal emission inside the dielectric where $\theta_i \geq \theta_C$ will be internally reflected at the dielectric-air interface when $n \gg 1$. Now, assume that the mirror is redesigned to follow Generalized Snell's Law of reflection. Now two cases are possible for thermal radiation generated in an internally reflected mode. In the first case, the angle will be reduced upon reflection. If the wavevector is increased by an appropriate amount, then the light may be reflected at an angle $|\theta_{r1}| < \theta_C$. More generally, after *N* bounces, it may be reflected at an angle $|\theta_{rN}| < \theta_C$. Such reflection angles inside the escape cone would allow the light to exit the high index medium. Alternatively, the angle will be increased upon reflection. However, after passing a certain threshold depicted on the right-hand side of Fig. 3(b), a secondary reflection will take place that will reverse the sign of the angle, reducing us to the first case.

Now consider the design parameters required to achieve the maximal emission enhancement. With an unlimited number of potential bounces, we merely need to ensure that the angle enters the escape cone once. The edge case is when the reflected angles are $\theta_{rN} = \theta_C$ and $\theta_{rN+1} = -\theta_C$ on the N$^{th}$ and N+1$^{th}$ bounces, respectively. This scenario requires $\delta = 2\sin\theta_C$, or $\Gamma_x = \lambda_0/2$. A smaller change in angles, and thus an acceptable result, could also be achieved if $\Gamma_x > \lambda_0/2$. For a range of wavelengths $(\lambda)$ close to $\lambda_0$, most of the wavelengths will couple out of the system, assuming that $\delta$ does not change. The precise bandwidth for this response will depend on the specifics of the design.

## DISCUSSION

A simple example of a mirror with the discussed properties is a graded refractive index layer on top of a conventional mirror. Neighboring sub-segments with different refractive indices have the same physical thickness and thus provide varying optical paths for the incoming wave. The phase added to the light wave by the sub-segments will vary according to the index gradient. Therefore as the wave goes through the graded index layer and returns to the medium of incidence, it will accumulate a spatial gradient phase $\Phi(x)$, which has to comply with the conditions discussed in the previous sub-section. The graded index layer must also be periodic and will have linearly varying indices ranging from $n_L$ to $n_H$. The mirror properties and the emission enhancement performance are discussed in the next section.

Now consider a graded index mirror embedded in a dielectric ($n = 3.5$). We introduce a matching layer on top of the graded index layer to minimize specular reflection (see Ref. [17] for details). We choose period $\Gamma_x = 1100$nm for the design wavelength $\lambda_0 = 1200$nm. The structure is uniform along y-direction. And, we only consider the $H_y$-polarization for the incident light. Although the (+1)-diffraction mode represents the desired $\theta_i - \theta_r$ relationship of the 'Generalized Snell's law of reflection', there are also other scattered modes. Note that the $\theta_i - \theta_r$ relationship predominantly follows the Generalized Snell's law of reflection for low $\theta_i$ (i.e., $|\theta_i| < 20°$). However, reflections at larger $\theta_i$ eventually revert to Snell's Law, i.e., specular reflection (with small contribution from other diffraction modes). No surface wave is observed for the high incidence angles—this is a deviation from the ideal characteristics. The angle of reflection for normal incidence $\theta_i = 0$ can be calculated for the (+1)-diffraction mode as follows:

$$\theta_r^{(+1)} = \text{asin}(\delta) = \text{asin}\left(\frac{\lambda/n}{\Gamma_x}\right) \tag{3}$$

For $\lambda = 1200$nm, $\Gamma_x = 1100$nm, and $n$ =3.5 we find $\theta_r^{(+1)} = 18.16°$, which matches with the numerical calculations. Also Eq. (3) predicts that $\theta_r^{(+1)}$ would increase with $\lambda$.

Now, consider a meta-surface mirror with a xylophone structure embedded in the dielectric, which behaves similarly to the graded index mirror structure (see Fig. 4(a)). Again, let the period $\Gamma_x = 1100$ nm and central wavelength $\lambda_0 = 1200$ nm. The $\theta_i - \theta_r$ relationship of the meta-mirror shows predominantly (+1)-diffraction (via Generalized Snell's Law) for small $\theta_i$, and returns to specular reflections for larger $\theta_i$. However, the meta-surface mirror is closer to the ideal case depicted in Fig. 3(b) [17].

**Selective Thermal Emission**

Next, let us focus on the enhancement of thermal emission using our proposed scheme. We can choose the dielectric thickness $L = 1.55$ mm (typical for a selective emitter substrate) on top of the xylophone meta-mirror structure, as shown in Fig. 4(a). To minimize reflections inside the escape cone, a quarter wave-matched (for $\lambda_0 = 1200$ nm) layer is used as an ARC. We choose a partially selective, weakly absorbing medium with refractive index $n = 3.5$, and a peak absorption coefficient $\alpha = 2$/cm. Both $n$ and $\alpha$ are assumed to be non-dispersive in the wavelength range of interest ($900 \text{ nm} < \lambda < 3000$ nm), to help achieve a better comparison of the emission enhancement properties. The blue and red lines in Fig. 4(b) show the angle-averaged absorptance for s- and p-polarizations respectively, for structures constructed using the meta-mirror configuration at the back. The baseline absorption doesn't experience enhancement, while the selective absorption range can be enhanced by the effect of photon trapping around 1500 nm. Therefore, the weak natural selective absorption of the substrate can be enhanced without increasing the absorption all over the spectrum. For the meta-mirror configuration in Fig. 4(a), there is minimal change in absorptance for $\lambda < \Gamma_x = 950$ nm, as predicted earlier. However, there are absorption peaks observed in this wavelength range. This can be associated with the resonances created by the series of dielectric layers. Also, note that the absorption starts to go down sharply for $\lambda > 1600$ nm, particularly with the s-polarization. Thus, the s-polarization offers the best overall selective thermal emission.

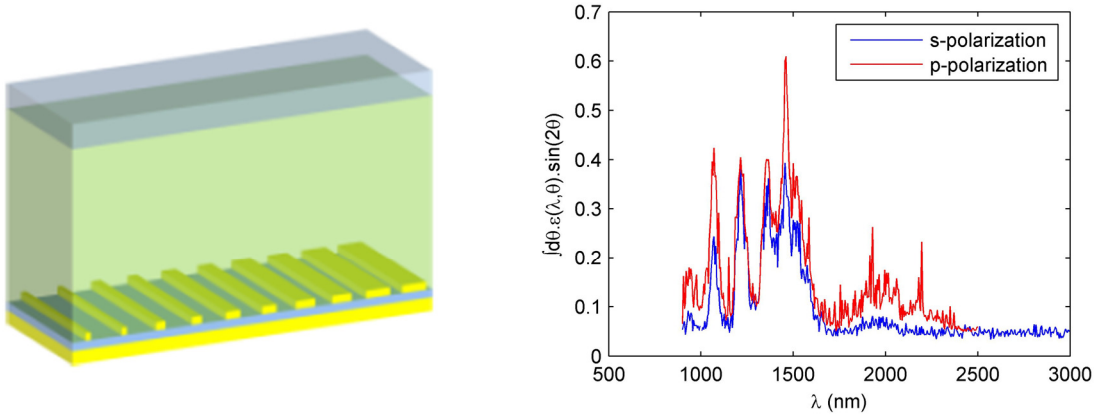


Fig. 4: (a) Xylophone meta-mirror structure for selective enhancement of thermal emission for a partially selective dielectric above with an anti-reflection coating on top. (b) Angle-averaged emissivity for s- and p-polarizations. The s-polarization shows particularly high selectivity for selective thermal emitter applications.

## CONCLUSIONS

In conclusion, this work has shown that ultrathin metasurfaces ($\boldsymbol{t < 20}$ nm) combined with ideal mirrors have tremendous potential for applications relying upon selective thermal emission, particularly including solar photovoltaics, selective solar absorption, thermophotovoltaics, and photon-enhanced thermionic emission. Two example meta-mirror structures were considered. The first example was a graded index and mirror, which showed angular deflections matching with analytical theory, albeit with performance approaching the conventional mirror at large angles. The second example using a xylophone metamirror structure showed stronger performance over a broad range of angles. This resulted in an enhancement of selective emission for both s- and p-polarized light at particular wavelengths in the infrared.

## ACKNOWLEDGMENTS

The authors thank Prof. V. Shalaev and Prof. A. Boltasseva for valuable discussions. This material is based upon work supported as part of the Center for Re-Defining Photovoltaic Efficiency Through Molecule Scale Control, an Energy Frontier Research Center funded by the U.S. Department of Energy, Office of Science, Office of Basic Energy Sciences under Award Number DE-SC0001085. The computational resources for this work were provided by the Network of Computational Nanotechnology under NSF Award EEC-0228390. This was also supported by the Bay Area PV Consortium, a Department of Energy project with Prime Award number DE-EE0004946.

**REFERENCES**


1. A.P. Raman, M.A. Anoma, L. Zhu, E. Rephaeli & S. Fan, "Passive radiative cooling below ambient air temperature under direct sunlight," Nature **515**, 540-544 (2014).
2. L. Zhu, A. Raman, K.X. Wang, M.A. Anoma & S. Fan, "Radiative cooling of solar cells," Optica **1**, 32-38 (2014).
3. L.T. Varghese, Y. Xuan, B. Niu, L. Fan, P. Bermel, & M. Qi, "Enhanced Photon Management of Thin-Film Silicon Solar Cells Using Inverse Opal Photonic Crystals with 3D Photonic Bandgaps," Adv. Opt. Mater. **1**, 692-698 (2013).
4. C. E. Kennedy, *Review of Mid- to High-Temperature Solar Selective Absorber Materials* (2002).
5. D. Chester, P. Bermel, J. D. Joannopoulos, M. Soljacic, and I. Celanovic, "Design and global optimization of high-efficiency solar thermal systems with tungsten cermets," Opt. Express **19**, A245–A257 (2011).
6. P. Bermel, W. Chan, Y. X. Yeng, J. D. Joannopoulos, M. Soljacic, and I. Celanovic, "Design and global optimization of high-efficiency thermophotovoltaic systems," Thermophotovoltaic World Conf. **9**, (2010).
7. J. W. Schwede, T. Sarmiento, V. K. Narasimhan, S. J. Rosenthal, D. C. Riley, F. Schmitt, I. Bargatin, K. Sahasrabuddhe, R. T. Howe, J. S. Harris, N. a Melosh, and Z.-X. Shen, "Photon-enhanced thermionic emission from heterostructures with low interface recombination.," Nat. Commun. **4**, 1576 (2013).
8. B. Wernsman, R. R. Siergiej, S. D. Link, R. G. Mahorter, M. N. Palmisiano, R. J. Wehrer, R. W. Schultz, G. P. Schmuck, R. L. Messham, S. Murray, C. S. Murray, F. Newman, D. Taylor, D. M. Depoy, and T. Rahmlow, "Greater Than 20% Radiant Heat Conversion Efficiency of a Thermophotovoltaic Radiator/Module System Using Reflective Spectral Control," IEEE Trans. Electron Devices **51**, 512–515 (2004).
9. E. Yablonovitch and G. D. Cody, "Intensity enhancement in textured optical sheets for solar cells," IEEE Trans. Electron Devices **ED-29**, 300–305 (1982).
10. T. Tiedje, E. Yablonovitch, G. D. Cody, and B. G. Brooks, "Limiting efficiency of silicon solar cells," IEEE Trans. Electron Devices **31**, 711–716 (1984).
11. P. Campbell and M. A. Green, "Light trapping properties of pyramidally textured surfaces," J. Appl. Phys. **62**, 243–249 (1987).
12. R. Brendel, *Thin-Film Crystalline Silicon Solar Cells* (Wiley-VCH, 2003).
13. N. Yu, P. Genevet, M. A. Kats, F. Aieta, J.-P. Tetienne, F. Capasso, and Z. Gaburro, "Light Propagation with Phase Reflection and Refraction," Science (80-. ). **334**, 333–337 (2011).
14. V. Liu and S. Fan, "S4 : A free electromagnetic solver for layered periodic structures," Comput. Phys. Commun. **183**, 2233–2244 (2012).
15. J. Kang, X. Wang, C. Liu, and P. Bermel, "S4: Stanford Stratified Structure Solver," (2013).
16. A. F. Oskooi, D. Roundy, M. Ibanescu, P. Bermel, J. D. Joannopoulos, and S. G. Johnson, "MEEP: A flexible free-software package for electromagnetic simulations by the FDTD method," Comp. Phys. Comm. **181**, 687–702 (2010).
17. M. R. Khan, X. Wang, P. Bermel, and M. A. Alam, "Enhanced light trapping in solar cells with a meta-mirror following generalized Snell's law," Opt. Express **22**, A973 (2014).